

Original article

**VISCOELASTIC PROPERTIES OF PASSIVE SKELETAL  
MUSCLE IN COMPRESSION: STRESS-RELAXATION  
BEHAVIOUR AND CONSTITUTIVE MODELLING**

M. Van Loocke, C.G. Lyons, C. K. Simms\*

*Centre for Bioengineering, Department of Mechanical and Manufacturing Engineering,  
Trinity College Dublin, Ireland*

Keywords: passive skeletal muscle, viscoelastic properties, compression, stress relaxation, quasi-linear viscoelastic model

Word count: 3643 (Introduction – Conclusions inclusive)

\*Corresponding author:

Centre for Bioengineering, Department of Mechanical and Manufacturing Engineering, Trinity College,  
Dublin 2, Ireland.

Tel.: +353-1-8963768. Fax: +353-1-6795554. Email: [csimms@tcd.ie](mailto:csimms@tcd.ie)

## Abstract

The compressive properties of skeletal muscle are important in impact biomechanics, rehabilitation engineering and surgical simulation. However, the mechanical behaviour of muscle tissue in compression remains poorly characterised. In this paper, the time-dependent properties of passive skeletal muscle were investigated using a combined experimental and theoretical approach. Uniaxial ramp and hold compression tests were performed *in vitro* on fresh porcine skeletal muscle at various rates and orientations of the tissue fibres. Results show that above a very small compression rate, the viscoelastic component plays a significant role in muscle mechanical properties; it represents approximately 50% of the total stress reached at a compression rate of  $0.5\%s^{-1}$ . A stiffening effect with compression rate is observed especially in directions closer to the muscle fibres. Skeletal muscle viscoelastic behaviour is thus dependent on compression rate and fibre orientation.

A model is proposed to represent the observed experimental behaviour which is based on the quasi-linear viscoelasticity framework. A previously developed Strain dependent Young's Moduli formulation was extended with Prony series to account for the tissue viscoelastic properties. Parameters of the model were obtained by fitting to stress-relaxation data obtained in the muscle fibre, cross-fibre and  $45^\circ$  directions. The model then successfully predicted stress-relaxation behaviour at  $60^\circ$  from the fibre direction (errors < 25%). Simultaneous fitting to data obtained at compression rates of 0.5, 1 and  $10\%s^{-1}$  was performed and the model provided a good fit to the data as well as good predictions of muscle behaviour at rates of 0.05 and  $5\%s^{-1}$  (errors < 25%).

## 1. Introduction

Virtual modelling is widely used in various biomechanical fields. Finite element models of the human body in compression are used in impact biomechanics (Forbes *et al.*, 2005 ; van Rooij *et al.*, 2003; Verver *et al.*, 2004); in rehabilitation engineering (Krouskop *et al.*, 1987; Linder-Ganz *et al.*, 2007; Mak *et al.*, 2001) and for simulation of surgical procedures (Guccione *et al.*, 2001; Keeve *et al.*, 1998). Such models require knowledge of body tissue mechanical properties. However, these are not well understood for soft tissues, especially when compressive loading is considered.

Skeletal muscle presents a complex fibre-oriented structure made of about 80% water, 3% fat and 10% collagenous tissues. It can therefore be expected to display time–and history dependent behaviour resulting from interactions between these constituents as shown for soft tissues with similar structure such as ligaments and tendons (Abramowitch *et al.*, 2004; Kwan *et al.*, 1993; Weiss *et al.*, 2002).

In a previous study (Van Loocke *et al.*, 2006), the elastic properties of passive skeletal muscle tissue were investigated by means of quasi-static uniaxial unconfined compression tests performed on fresh porcine muscle tissue *in vitro*. Results showed that muscle elastic behaviour is nonlinear and transversely isotropic; the stiffest direction being the cross-fibre direction, followed by the fibre and the 45° directions respectively. A transversely isotropic model including Strain dependent Young's Moduli (SYM) was developed which successfully fitted experimental data and also yielded excellent predictions of muscle compressive behaviour in various orientations of the muscle fibres.

This paper addresses the viscoelastic behaviour of muscle tissue and complements the information provided in Van Loocke *et al.*, 2006 on the fundamental mechanical behaviour of skeletal muscle in compression.

As pointed out previously (Palevski *et al.*, 2006), there is little published data on skeletal muscle viscoelastic properties (Best *et al.*, 1994 in tension; Bosboom *et al.*, 2001a,b in compression). Indentation tests have been performed by some authors on skeletal muscle (Gefen *et al.*, 2005; Palevski *et al.*, 2006; Zheng *et al.*, 1999). However, these have considered muscle tissue as isotropic and as having linear elastic and viscoelastic properties.

In this paper stress-relaxation tests performed on fresh porcine muscle tissue are reported and a constitutive model is proposed. Fibre orientation, strain levels and strain rates were varied to determine their influence on the viscoelastic properties of muscle in compression (anisotropy and nonlinearity). We have previously shown that the hypothesis of strain dependent transverse isotropy yields a model which provides a very good fit and predictive capabilities for muscle tissue compression up to 30% strain. In this paper it is hypothesised that this model can be extended using the quasi-linear viscoelasticity framework (Fung, 1993) formulated with Prony series to predict the large strain three-dimensional relaxation behaviour of muscle tissue in compression.

## **2. Materials and methods**

The experimental protocol applied during the tests presented in this paper is very similar to the protocol applied for previous quasi-static testing of porcine muscle tissue (Van Loocke *et al.*, 2006). Uniaxial unconfined compression tests were performed on fresh porcine muscles excised from the pelvic limb (gluteus muscle) of male pigs aged 10-12 weeks. From the belly of these muscles, cubic samples oriented in the fibre (F) and cross-fibre (XF) directions and at 45° and 60° from the fibre direction were cut and kept at room temperature in airtight containers prior to testing, which was completed within three hours post-mortem in order to avoid *rigor mortis* effects (Van Loocke *et al.*, 2006). The samples had characteristic dimensions between 5 and 10mm (measurement made with vernier calipers). Six animals were used for the tests conducted on a Zwick Z005 machine (Zwick GmbH & Co. Ulm, Germany). Force and displacement were recorded with a time resolution of 0.05s. Samples were compressed up to 30% strain at rates of 0.5, 1, 5 and 10% $s^{-1}$ . Following the ramp, compression was held constant for 300s to allow for relaxation. Six samples were tested in each direction (F, XF, 45° and 60°). Each sample was tested once as the high strain level leads to some permanent tissue deformation and no preconditioning was applied to the samples for the same reason. Given the short duration of the tests (360s at most), dehydration of the samples was not an issue. Similar tests were also performed with peak compression levels of 10% and 20% at a rate of 1% $s^{-1}$ . During these tests, six samples were tested in fibre and cross-fibre directions.

### **3. Experimental results**

The deformation applied to the samples consisted of ramp and hold functions and results from both parts of the deformation history are examined separately. Mean experimental results are presented using Cauchy stress and stretch ratio. Results presented correspond to means calculated from six samples tested for each type of test and each fibre orientation.

#### **3.1. Influence of deformation rate and fibre orientation on muscle compressive behaviour**

This section focuses on the ramp portion of the tests. Figure 1 presents experimental stress-stretch ratio curves obtained at various rates and fibre orientations. Results at  $0.05\%s^{-1}$  are the quasi-static tests presented in Van Loocke *et al.*, 2006. As expected, a stiffening effect with compression rate is always observed, but this is more significant in directions closer to the fibre direction. Figure 2 shows the dependence of stress on compression rate at 30% compression, for the fibre orientations considered. During quasi-static tests ( $0.05\%s^{-1}$ ), the cross-fibre direction is much stiffer than the fibre direction (ratio of 1.76 at 30% compression). However, as compression rate increases, the difference in stiffness between both directions diminishes. At  $5\%s^{-1}$  the trend is inverted and the fibre direction is then stiffer than the cross-fibre direction.

#### **3.2. Influence of deformation rate and fibre orientation on muscle stress relaxation behaviour**

This section considers relaxation behaviour during constant compression following the ramp. Figure 3 compares mean stress-relaxation curves obtained at various compression rates and fibre orientations. Significant stress-relaxation occurs when deformation is held constant after a compressive ramp, especially within the first hundred seconds of relaxation. Table 1 reports mean values of stress after 300s relaxation and results from previous quasi-static tests are also shown. For each fibre orientation, differences are observed between relaxed values reached at various rates. However, a one-way ANOVA shows that most of the relaxed values are not significantly different from each other. These differences might therefore be attributed to intra-specimen variability which leads us to believe that muscle relaxation behaviour is independent of compression rate. For each fibre direction considered, a mean relaxed muscle state is defined as the mean between relaxed values obtained at various rates (final

column in table 1). These relaxed values are smaller than quasi-static values for most tests but analysis shows that significant differences appear only in the cross-fibre direction. This will be addressed further in the discussion.

The peak stress reached after the ramp ( $\sigma_{tot}$ ) can be considered as the sum of a long term elastic ( $\sigma_e$ ) and a viscoelastic contribution ( $\sigma_v$ ). The relative contribution of the viscoelastic component is:

$$\frac{\sigma_v}{\sigma_{tot}} = \frac{\sigma_{tot} - \sigma_e}{\sigma_{tot}} \quad (1)$$

Figure 4 presents the  $\sigma_v/\sigma_{tot}$  ratios calculated at 30% compression for the deformation rates applied. These ratios were calculated using the mean values obtained after relaxation for the elastic stress. An increase in compression rate leads to an increase in the viscoelastic contribution to the total stress and the viscoelastic component has a greater influence in directions closer to the muscle fibres. A relatively minor viscoelastic contribution to the stress obtained from quasi-static testing can be observed due to the differences observed between quasi-static and relaxed values (differences of 2.8 and 18% respectively in fibre and cross-fibre directions).

### 3.3. Evolution of muscle stress relaxation behaviour with compression level

Figure 5 presents results from relaxation tests performed in the fibre and cross-fibre directions up to 10%, 20% and 30% compression at a compression rate of  $1\%s^{-1}$ . The cross-fibre direction remains stiffer than the fibre direction and a substantial stress relaxation is observed at all compression levels. Power regression of stress relaxation of the form

$$\sigma(t) = \exp(a) t^m, \quad (2)$$

where  $a$  and  $m$  are parameters of fit, shows a linear relationship, aside from the initial relaxation response in the first 10 seconds, see figure 6. The parameter  $m$  is the rate of relaxation which increases when the level of compression decreases. A one-way ANOVA indicates that statistically significant differences between values of  $m$  appear only in the fibre direction. However, the results indicate that muscle relaxation behaviour is dependent on deformation level.

## 4. Constitutive modelling

A transversely isotropic, Strain dependent Young's Moduli (SYM model) model was previously developed to represent skeletal muscle nonlinear elastic properties (Van Loocke *et al.*, 2006). See Appendix. In this paper, a discretised quasi-linear viscoelastic approach (Fung, 1993) was followed and the SYM model was extended with Prony series to represent skeletal muscle viscoelastic behaviour.

### 4.1. Quasi-linear viscoelastic SYM model – Unidirectional approach

A unidirectional approach was first investigated; fitting of the model to the experimental data was performed individually for each orientation of the muscle fibres considered. The Cauchy stress in direction  $j$  can be expressed as:

$$\sigma_j(t) = \sigma_j^e(0+)G_j(t) + \int_0^t G_j(t-\tau) \frac{\partial \sigma_j^e[\tilde{\epsilon}_j(\tau)]}{\partial \tau} d\tau \quad (3)$$

where  $G_j(t)$  is the reduced relaxation function and  $\sigma_j^e$  the instantaneous elastic stress and logarithmic strains are adopted to account for large deformations,  $\tilde{\epsilon}_j = \ln(\lambda_j)$ . Using a Prony series expansion for

the reduced relaxation function,  $G_j(t) = p_{\infty j} + \sum_{i=1}^N p_{ij} \exp(-\frac{t}{\tau_{ij}})$  leads to:

$$\sigma_j(t) = p_{\infty j} \sigma_j^e(t) + \sum_{i=1}^N \int_0^t p_{ij} \exp\left(-\frac{(t-\tau)}{\tau_{ij}}\right) \frac{\partial \sigma_j^e[\tilde{\epsilon}_j(\tau)]}{\partial \tau} d\tau \quad (4)$$

where  $p_{ij}$  and  $\tau_{ij}$  characterise the viscoelastic behaviour in direction  $j$ ;  $p_{\infty j} = 1 - \sum_{i=1}^N p_{ij}$ .

The SYM formulation was then introduced for the long term elastic stress,  $\sigma_{\infty j} = p_{\infty j} \sigma_j^e = k_{1j} \tilde{\epsilon}_j + k_{2j} \tilde{\epsilon}_j^2 + k_{3j} \tilde{\epsilon}_j^3$ ;  $k_{1j}$ ,  $k_{2j}$  and  $k_{3j}$  are SYM model parameters (Van Loocke *et al.*, 2006). The time evolution of this model was implemented using a numerical integration procedure developed by Goh *et al.* (2004). Simultaneous fitting to data obtained at various rates was performed in order to obtain a global set of parameters representative of muscle relaxation behaviour in a given direction. A five term Prony series was adopted for the viscoelastic formulation. Ten parameters were

determined for each orientation,  $p_{1j,\dots,5j}$  and  $\tau_{1j,\dots,5j}$ , using the Matlab function *lsqnonlin* and the complete deformation history was used in the regression.

A first fitting to the data showed that the five time constants ( $\tau_{ij}$ ) characterising muscle relaxation behaviour ranged from 0.6 to 300s. To reduce the number of variables, these were therefore fixed at 0.6, 6, 30, 60 and 300s, independently of deformation rate or fibre orientation. The five remaining parameters are the multiplicative factors ( $p_{ij}$ ) characterising the amplitude of each viscoelastic component and were obtained by simultaneous fitting to experimental data obtained at compression rates of 0.5, 1 and 10% $s^{-1}$ . Figures 7 and 8 present regression results in the fibre and cross-fibre directions; similar results were obtained in the two other directions. Bearing in mind that variability is observed within experimental data, the model provides a very good fit to data obtained at a compression rate of 0.5, 1 and 10% $s^{-1}$  as well as a good prediction of muscle behaviour at 0.05 and 5% $s^{-1}$ .

Figure 9 compares (a) relaxed and (b) peak values of experimental and theoretical stress, obtained in the cross-fibre direction. Minimum, maximum and median experimental values are presented. Figure 9(a) illustrates the variability present in the experimental relaxed stresses. As stated, the model relaxes independently of compression rate to a unique value situated in the middle of the range of relaxed stresses observed experimentally. This explains why small differences appear between experimental and theoretical relaxed values of stress. Analysis shows that percentage errors between experimental and theoretical relaxed or peak stresses remain below 25% at all rates and fibre orientations considered (Figure 10).

#### 4.2. Quasi-linear viscoelastic SYM model – Introduction of fibre dependency

Individual fitting to relaxation data from various fibre orientations showed that the  $p_{ij}$  factors are fibre-direction dependent due to tissue anisotropy. Using an approach similar to that adopted for muscle elastic properties (Van Loocke *et al.*, 2006), it was therefore hypothesised that muscle viscoelastic properties are also transversely isotropic. Replacing the instantaneous elastic stress by the long term elastic stress in equation (4), the stress in direction  $j$  can be expressed as:

$$\sigma_j(t) = \sigma_{\infty j}(t) + \sum_{i=1}^N \int_0^t \frac{p_{ij}}{p_{\infty j}} \exp\left(-\frac{(t-\tau)}{\tau_{ij}}\right) \frac{\partial \sigma_{\infty j}[\tilde{\epsilon}_j(\tau)]}{\partial \tilde{\epsilon}_j(\tau)} \frac{\partial \tilde{\epsilon}_j(\tau)}{\partial \tau} d\tau \quad (5)$$



or

$$\sigma_j(t) = E_j \tilde{\epsilon}_j(t) + \int_0^t E_j^v \frac{\partial \tilde{\epsilon}_j(\tau)}{\partial \tau} d\tau \quad (6)$$

where  $E_j = k_{1j} + k_{2j} \tilde{\epsilon}_j + k_{3j} \tilde{\epsilon}_j^2$ , represents the elastic Young's modulus in direction  $j$  and

$$E_j^v = \sum_{i=1}^5 \frac{p_{ij}}{p_{\infty j}} \exp\left(\frac{-(t-\tau)}{\tau_{ij}}\right) \frac{\partial \sigma_{\infty j}[\tilde{\epsilon}_j(\tau)]}{\partial \tilde{\epsilon}_j(\tau)},$$

is the viscoelastic Young's modulus in direction  $j$ .

$E_L^v$  and  $E_T^v$  were determined by fitting to stress-relaxation data obtained respectively in the fibre and in the cross-fibre directions in the same manner as the equivalent elastic parameters (Van Loocke *et al.*, 2006). Similarly, the viscoelastic shear modulus  $G_{LT}^v$  was calculated using data obtained at 45° from the fibre direction and:

$$\frac{1}{G_{LT}^v} = \frac{4}{E_{45}^v} - \frac{1-2\nu_{LT}}{E_L^v} - \frac{1}{E_T^v} \quad (7)$$

The viscoelastic Young's modulus at any angle ( $\omega$ ) from the fibre direction was found from:

$$\frac{1}{E_\omega^v} = \frac{1}{E_L^v} \cos^4 \omega + \left( \frac{1}{G_{LT}^v} - 2 \frac{\nu_{LT}}{E_L^v} \right) \sin^2 \omega \cos^2 \omega + \frac{1}{E_T^v} \sin^4 \omega \quad (8)$$

Comparison between experimental results and theoretical values calculated with  $\omega = 60^\circ$  are presented in figure 11.

Results show that model predictions are in good agreement with experimental stress-relaxation data obtained at 60° from the fibre direction; errors between experimental and theoretical peak and relaxed stresses remain below 10% in most cases considered (Figure 12). These results indicate that anisotropy observed in muscle viscoelastic behaviour can be captured by the transversely isotropic viscoelastic model developed.

## 5. Discussion

In this paper, the stress relaxation behaviour of skeletal muscle tissue was experimentally investigated and a constitutive model is proposed to represent this behaviour. Results from ramp and hold tests performed at various rates and fibres orientations showed that above a very small compression rate, the viscoelastic component ( $\sigma_v$ ) plays a significant role on muscle mechanical properties ( $\sigma_v$  represents 49%

of the total stress in cross-fibre direction at a compression rate of  $0.5\%s^{-1}$ ). A substantial amount of stress-relaxation occurred when deformation was held constant after a compressive ramp: over 45% and over 60% stress-relaxation are respectively observed in the cross-fibre and fibre directions for tests performed at  $0.5\%s^{-1}$ . The data also show that over 80% of the total relaxation occurs within 100s. A stiffening effect with compression rate was also observed in all directions of testing. However, the increase in stiffness with compression rate is more significant in directions closer to the fibre direction. Skeletal muscle compressive behaviour is thus dependent on compression rate and fibre orientation. Results also indicate that muscle relaxation behaviour is independent of compression rate. A dependency on compression level was however observed; the rate of relaxation increased approximately by 20% when the maximum compression level decreased from 30 to 10% deformation.

The quasi-linear viscoelastic theory developed by Fung remains the most widely used approach to represent soft tissue viscoelasticity. The applicability of this model in a discretised form to represent skeletal muscle viscoelastic properties was therefore investigated. The model proposed is an extension with Prony series of the SYM model, which successfully represents the nonlinear elastic, transversely isotropic properties of muscle tissue in quasi-static compression (Van Loocke *et al.*, 2006). Using a similar approach as for muscle elastic properties, it was hypothesised that muscle viscoelastic properties are also transversely isotropic. Model parameters were obtained by fitting to stress-relaxation data obtained in the fibre, cross-fibre and the  $45^\circ$  direction and the model was then successfully used to predict stress-relaxation behaviour at  $60^\circ$  from the fibre direction (see figure 11). Results also show that the model provides a good fit to the data considered as well as a good prediction of muscle behaviour at rates of 0.05 and  $5\%s^{-1}$  (see figures 7 and 8).

The literature on muscle viscoelastic behaviour is sparse but it does confirm that skeletal muscle compressive properties depend on the deformation rate. Quantitative comparisons are however difficult to establish due to differences in the experimental protocols used. Bosboom *et al.* (2001b) presented results of ramp and hold compression tests conducted *in vivo* on rat tibialis anterior (TA) muscles in the transverse direction. However, they used a hold phase of only 20s and the relaxation behaviour could thus not be fully captured. These data were fitted with an isotropic viscoelastic hyperelastic model,

including a single term Prony series with a time constant of 6.01s which corresponds well to one of the five time constants reported here.

Palevski *et al.* (2006) performed rapid indentation tests on fresh porcine gluteus muscle *in vitro* to measure the transient shear modulus ( $G(t)$ ) of the tissue in the transverse direction. Short term ( $G_S$ ) and long term ( $G_L$ ) shear moduli were obtained from the experiments and  $G(t)$  data were fitted to a biexponential equation. A hold phase of 60s only was considered in these experiments to capture the long term properties of the tissue; our tests show however that relaxation still occurs after a hold phase of 300s. Palevski *et al.* considered muscle tissue as an isotropic linear elastic material and a value of  $\sim 700 \pm 300$  Pa is reported in the paper for  $G_L$  of skeletal muscle in the transverse direction. However, previous research clearly shows that muscle elastic behaviour is nonlinear (Grieve and Armstrong, 1988; McElhaney, 1966; Van Looke *et al.*, 2006; Van Sligtenhorst *et al.*, 2006). To establish a comparison with our nonlinear data, an average value was calculated for the long term shear modulus in the transverse direction. A value of 523 Pa was obtained, which is in good agreement with the data from Palevski *et al.*

*In vivo* indentation tests have also been performed on human bulk muscular tissues. Zheng *et al.* (1999) used indentation rates ranging approximately from 4 to 40% $s^{-1}$  and reported that the tissue properties appeared to be rate-insensitive in the range tested. This contradicts our findings which show a clear dependency of muscle compressive behaviour to compression rate. Silver-Thorn *et al.* (1999) reported that limb bulk soft tissues undergo substantial relaxation: after indenting the tissue at 5mm. $s^{-1}$ , 95% relaxation was observed on average, most of it within five seconds. These are higher than the values observed during our tests in which approximately 50% relaxation was obtained in the cross-fibre direction and 80% of this amount occurred in the first 100s. However, indentation tests measure bulk muscular properties (skin, fat and muscle tissue combined), and may not be valid for a large deformations. Furthermore, muscle activity was only assessed qualitatively in the tests and all of these factors could influence the results and explain the differences observed.

Grieve and Armstrong (1988) performed *in vitro* measurements of aged porcine muscle tissues compressive properties and also observed an increase in stiffness with compression rate. The stress

reached after 30% compression is approximately doubled from 0.05 to 2.5; which is similar to the observations made in this study.

McElhaney (1966), Van Sligtenhorst *et al.* (2006), Song *et al.* (article in press) observed that muscle compressive response is nonlinear and strongly strain-rate sensitive. However, very high compression levels (up to 80%) and strain rates (up to  $3700\text{s}^{-1}$ ) were considered in these studies, and the presentation of the data does not allow a direct comparison with the data obtained in this study.

To explain the greater influence of the viscoelastic component in directions closer to the muscle fibres, a possible explanation is hypothesised. Noting no expulsion of fluid from the specimens during the tests, and that cross fibre expansion occurs during fibre direction compression, muscle tissue might be considered as made of fluid filled fibre fascicles surrounded by connective tissue which constrains the flow of fluid (Figure 13). The movement of the fluid component appears to be easier along the direction of the fibres than across their direction. When compression takes place in the cross-fibre direction (a), the fluid is free to rearrange itself; whereas during compression in the fibre direction (b), the fluid is further constrained by the endomysium and perimysium layers. This unverified hypothesis remains speculative and requires further investigation.

The experimental procedure used in this study presents some limitations. A critical point in the measurement of a materials' relaxation behaviour is the choice of the cut-off time for the experiment. The values of stress reached after 300s were here considered as steady-state, relaxed values even though a small amount of relaxation still occurred after the end of the tests. However, the 300s allowed for relaxation was considered as a good compromise between measurement of "truly relaxed" muscle properties and test duration which was limited by the onset of rigor mortis a few hours after death leading to stiffer mechanical properties (Van Loocke *et al.*, 2006).

Small differences were also observed between values of stress obtained during quasi-static tests and values of stress obtained from ramp and hold tests, after relaxation. These values should ideally be the same as they both correspond to the long term elastic properties of the tissue. Differences indicate that the compression rate adopted for quasi-static tests was not low enough to measure only purely elastic properties. However, as stated,  $0.05\%s^{-1}$  was chosen as a compromise between test duration and measurement of long term elastic properties of the tissue.

A limitation of the model proposed appears in the prediction of muscle relaxation behaviour at various strain levels. Results from relaxation tests performed at 10, 20 and 30% compression indicate that the rate of relaxation increases when the level of compression decreases. This phenomenon is not captured by the model; however, the magnitude of the theoretical results remains close to experimental data.

## **6. Conclusions**

Compressive tests performed on fresh porcine muscle demonstrate that the viscoelastic component plays a significant role in muscle mechanical behaviour from a very low compression rate. Viscoelastic properties must therefore be taken into account when modelling the tissue behaviour, even in applications where strain rates remain small (e.g. modelling of surgical procedures). Results also show that the influence of the viscoelastic component is greater in directions closer to the muscle fibres; skeletal muscle therefore also presents anisotropic viscoelastic behaviour. A nonlinear elastic transversely isotropic model extended with Prony series reproduces the observed experimental behaviour very well and is appropriate to represent skeletal muscle stress-relaxation behaviour at the rates considered. The predictive capabilities of the model when muscle is subjected to higher loading rates requires a suitable experimental protocol and will be a future focus of our research. Such tests at higher compression rates would fill the gap between data presented in this paper and those data published in the literature at very high compression rates (McElhaney, 1966; Van Sligtenhorst *et al.*, 2006; Song *et al.*, In Press).

## **Acknowledgements**

This project is funded by the Programme for Research in Third Level Institutions (PRTL), administered by the Irish Higher Education Authority (HEA).

## **References**

Abramowitch, S. D., Woo, S. L. Y., Clineff, T. D., Debski, R. E., 2004. An evaluation of the quasi-linear viscoelastic properties of the healing medial collateral ligament in a goat model. *Annals of Biomedical Engineering* 32, 329-335.

Best, T.M., McElhaney, J., Garrett, Jr W.E., Myers, B.S., 1994. Characterization of the passive responses of live skeletal muscle using the quasi-linear theory of viscoelasticity. *Journal of Biomechanics* 27, 413-419.

Bosboom, E.M.H., Thomassen, J.A.M., Oomens, C.W.J., Bouten, C.V.C., Baaijens, F.P.T., 2001a. A numerical experimental approach to determine the transverse mechanical properties of skeletal muscle. In: Middleton, J., Jones, M.L., Shrive, N.G. (Eds.), *Computer Methods in Biomechanics and Biomedical Engineering-3*. pp. Gordon and Breach Sciences Publishers, 187-192.

Bosboom, E.M.H., Hesselink, M.K.C., Oomens, C.W.J., Bouten, C.V.C., Drost, M.R, Baaijens, F.P.T., 2001b. Passive transverse mechanical properties of skeletal muscle under in vivo compression. *Journal of Biomechanics* 34, 1365-1368.

Forbes, P.A., Cronin, D.S., Deng, Y.C., Boismenu, M., 2005. Numerical human model to predict side impact thoracic trauma. In: Gilchrist, M.D. (Ed.), *IUTAM Symposium on Impact Biomechanics: From Fundamental Insights to Applications*. Springer, pp. 441-450.

Fung, Y. C., 1993. *Biomechanics: Mechanical properties of living tissues*. Springer-Verlag, New York.

Gefen, A., Gefen, N., Linder-Ganz, E., Margulies, S. S., 2005. *In Vivo* muscle stiffening under bone compression promotes deep pressure sores. *Journal of Biomechanical Engineering* 127, 512-524.

Goh, S. M., Charalambides, M. N., Williams, J. G., 2004. Determination of the constitutive constants of non-linear viscoelastic materials. *Mechanics of Time-Dependent Materials* 8, 255-268.

Grieve, A. P., Armstrong, C. G., 1988. Compressive properties of soft tissues. In: de Groot, G., Hollander, A. P., Huijing, P. A., van Ingen Schenau, G. J. (Eds.), *Biomechanics XI-A. International series on biomechanics*. Free University Press, Amsterdam, pp. 531-536.

Guccione, J. M., Moonly, S. M., Wallace, A. W., Ratcliffe, M. B., 2001. Residual stress produced by ventricular volume reduction surgery has little effect on ventricular function and mechanics: a finite element model study. *Journal of Thoracic and Cardiovascular Surgery* 122, 592-599.

Keeve, E., Girod, S., Kikinis, R., Girod, B., 1998. Deformable Modeling of Facial Tissue for Craniofacial Surgery Simulation. *Computer Aided Surgery* 3, 228-238.

Krouskop, T. A., Muilenberg, A. L., Dougherty, D. R., Winningham, D. J., 1987. Computer-aided design of a prosthetic socket for an above-knee amputee. *Journal of Rehabilitation Research and Development* 24, 31-38.

Kwan, M. K., Lin, T. H., Woo, S. L., 1993. On the viscoelastic properties of the anteromedial bundle of the anterior cruciate ligament. *Journal of Biomechanics* 26, 447-52.

Linder-Ganz, E., Shabshin, N., Itzchak, Y., Gefen, A., 2007. Assessment of mechanical conditions in sub-dermal tissues during sitting: A combined experimental-MRI and finite element approach. *Journal of Biomechanics* 40, 1443-1454.

Mak, A. F. T., Zhang, M., Boone, D. A., 2001. State-of-the-art research in lower-limb prosthetic biomechanics-socket interface. *Journal of Rehabilitation Research and Development* 38(2), .

McElhaney, J. H., 1966. Dynamic response of bone and muscle tissue. *Journal of Applied Physiology* 21, 1231-1236.

Palevski, A., Ittai Glai, I., Portnoy, S., Linder-Ganz, E., Gefen, A., 2006. Stress Relaxation of Porcine Gluteus Muscle Subjected to Sudden Transverse Deformation as Related to Pressure Sore Modeling. *Journal of Biomechanical Engineering* 128(5), 782-787.

Silver-Thorn, M. B., 1999. In Vivo indentation of lower extremity limb soft tissues. *IEEE Transactions on Rehabilitation Engineering* 7(3), 268-277.

Song, B., Chen, W., Weerasooriya, T. Dynamic and quasi-static compressive response of porcine muscle. *Journal of Biomechanics*, Article in Press.

Tschoegl, N. W., 1989. The phenomenological theory of linear viscoelastic behavior: an introduction. Springer, Berlin, 1989.

Van Sligtenhorst, C., Cronin, D. S., Wayne Brodland, G., 2006. High strain rate compressive properties of bovine muscle tissue determined using a split Hopkinson bar apparatus. *Journal of Biomechanics* 39, 1852-1858.

van Rooij, L., Bours, R., van Hoof, J., Mihm, J. J., Ridella, S. A., Bass, C. R., Crandall, J. R., 2003. The development, validation and application of a finite element upper extremity model subjected to airbag loading. *Stapp Car Crash Journal*, 47.

Van Loocke, M., Lyons, C. G., Simms, C. K., 2006. A validated model of passive muscle in compression. *Journal of Biomechanics* 39(16), 2999-3009.

Verver, M. M., van Hoof, J., Oomens, C. W. J., Wismans, J. S. H. M., Baaijens, F. P. T., 2004. A finite element model of the human buttocks for prediction of seat pressure distributions. *Computer Methods in Biomechanics and Biomedical Engineering* 7, 193-203.

Weiss, J. A., Gardiner, J. C., Bonifasi-Lista, C., 2002. Ligament material behavior is nonlinear, viscoelastic and rate-independent under shear loading. *Journal of Biomechanics* 35, 943-950.

Zheng, Y., Mak, A. F.T., Lue, B., 1999. Objective assessment of limb tissue elasticity: Development of a manual indentation procedure. *Journal of Rehabilitation Research and Development* 36, 2.



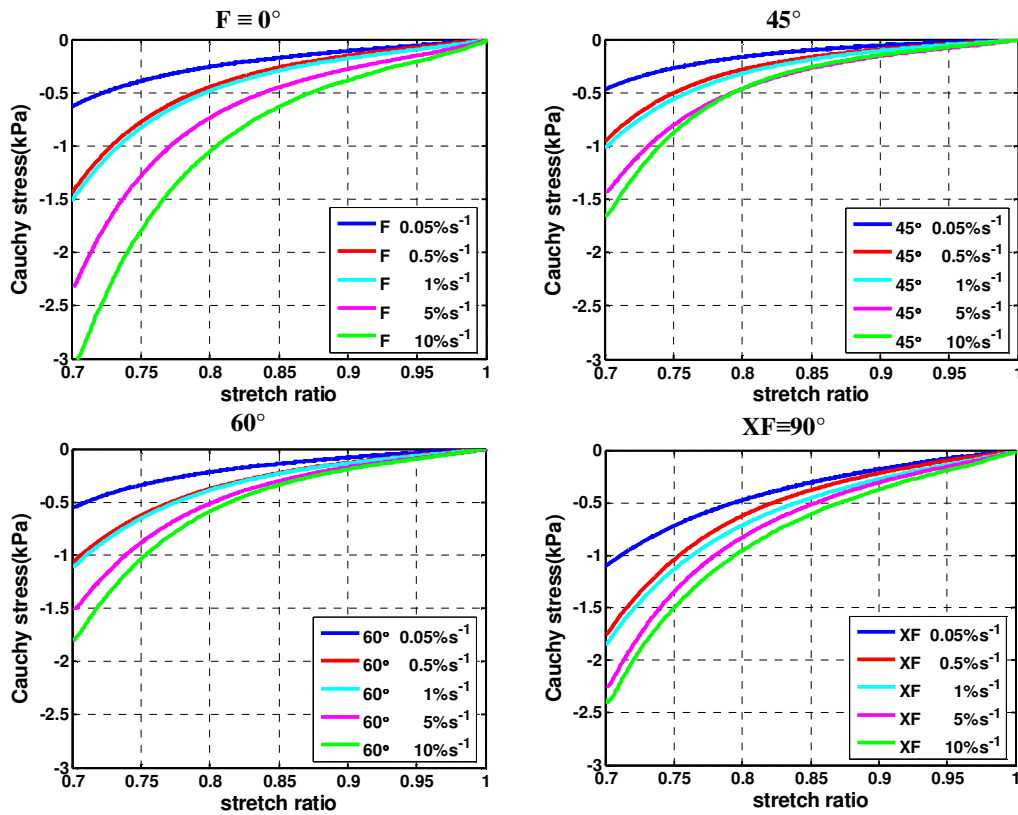


Figure 1: Stress-stretch curves comparing porcine muscle compressive behaviour at various rates (0.05, 0.5, 1, 5 and 10% $s^{-1}$ ) and various orientations of the muscle fibres (fibre  $\equiv 0^\circ$ ,  $45^\circ$ ,  $60^\circ$  and cross-fibre  $\equiv 90^\circ$  from the fibre direction).

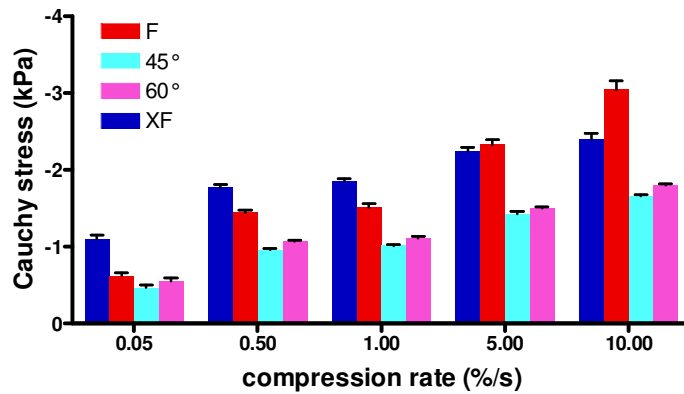


Figure 2: Dependence of stress on compression rate at 30% compression in various orientations of the muscle fibres. Mean values with standard deviations.

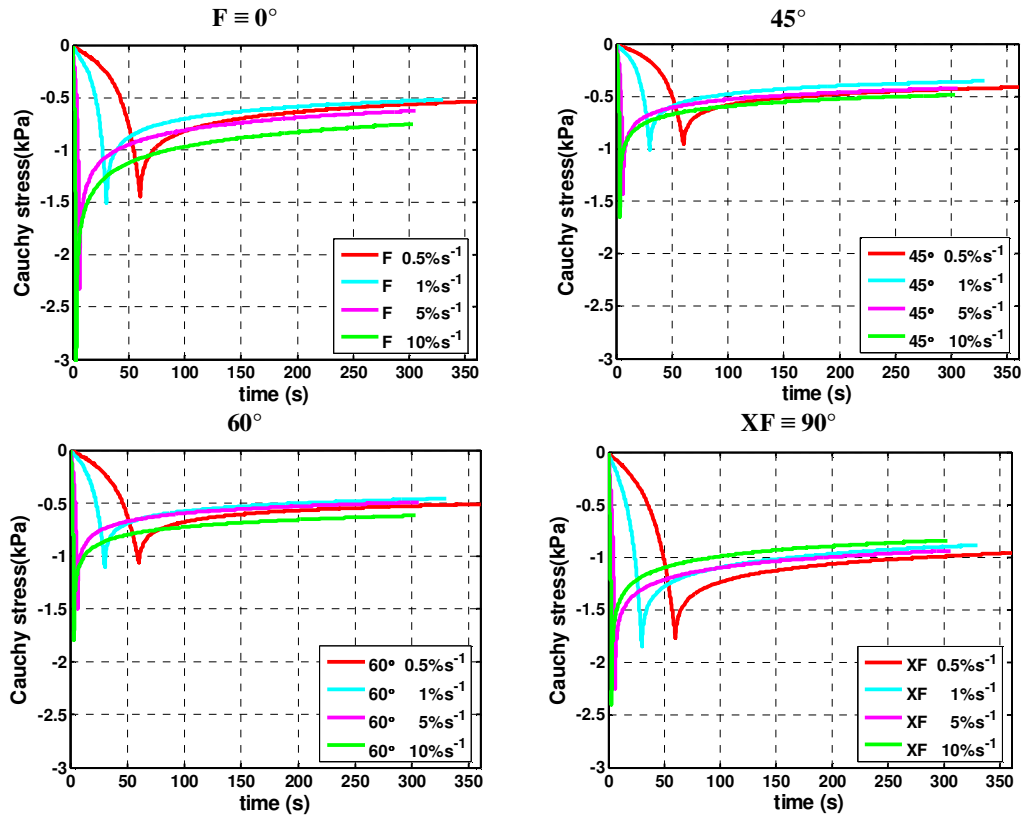


Figure 3: Stress-relaxation curves obtained at various compression rates (0.05, 0.5, 1, 5 and 10% s<sup>-1</sup>) and various orientations of the muscle fibres (fibre ≡ 0°, 45°, 60° and cross-fibre ≡ 90° from the fibre direction).

Table 1: Values of stress at 30% compression in quasi-static and relaxation tests (values taken after 300s relaxation) - stress±SD (kPa)

	Quasi-static tests	Relaxation tests				Mean value
	0.05% s <sup>-1</sup>	0.5% s <sup>-1</sup>	1% s <sup>-1</sup>	5% s <sup>-1</sup>	10% s <sup>-1</sup>	
F	-0.63±0.14	-0.54±0.04	-0.52±0.04	-0.62±0.06	-0.75±0.12	-0.61±0.11
45°	-0.47±0.15	-0.41±0.02	-0.35±0.02	-0.42±0.02	-0.48±0.06	-0.42±0.05
60°	-0.55±0.14	-0.51±0.04	-0.46±0.03	-0.49±0.06	-0.62±0.03	-0.52±0.07
XF	-1.10±0.17	-0.96±0.05	-0.88±0.03	-0.94±0.09	-0.84±0.04	-0.90±0.05

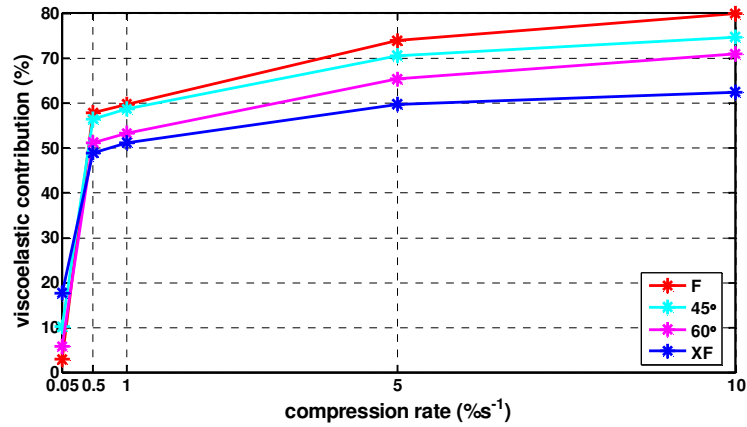


Figure 4: Relative contribution of the viscoelastic component to the total stress reached at 30% compression at various strain rates and fibre orientations. Values obtained using equation (1) with  $\sigma_e$  = mean relaxed values.

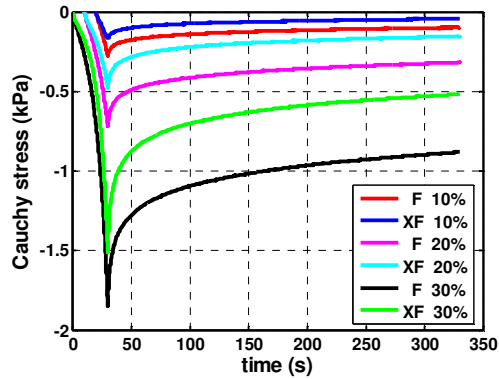


Figure 5: Stress relaxation curves in fibre and cross-fibre directions after 10, 20 and 30% compression at a rate of  $1\% s^{-1}$ .

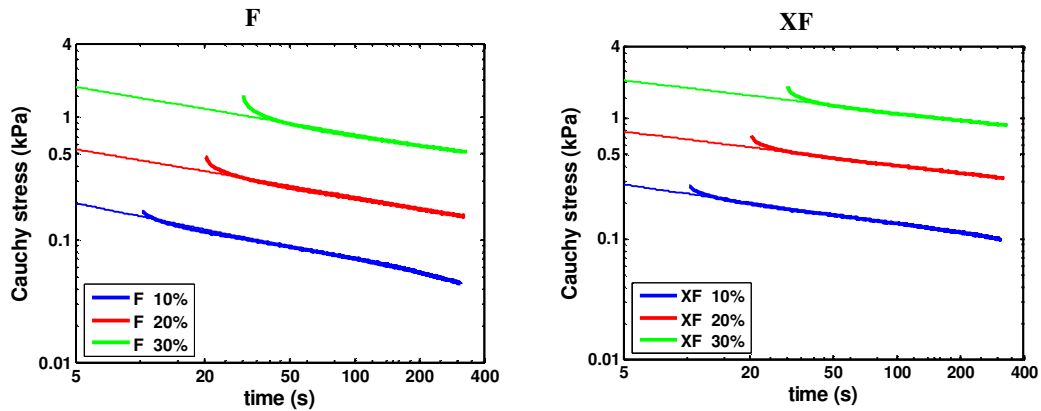


Figure 6: Stress-relaxation curves on logarithmic scales illustrating the linear trend of the stress decay. Thick lines represent experimental results; thin lines represent power-law fitting.

Table 2: Parameters  $m$  for power-law fitting of stress-relaxation curves obtained at various levels of compression in fibre and cross-fibre directions.

		10%	20%	30%
$m$	F	$-0.356 \pm 0.045$	$-0.298 \pm 0.019$	$-0.298 \pm 0.018$
	XF	$-0.252 \pm 0.048$	$-0.217 \pm 0.032$	$-0.208 \pm 0.015$

Fibre direction

Parameters values				
$K_{1L}$ (kPa)	$k_{2L}$ (kPa)	$k_{3L}$ (kPa)	-	-
1.005	2.989	10.985		
$p_{1L}$	$p_{2L}$	$p_{3L}$	$p_{4L}$	$p_{5L}$
0.465	0.200	0.057	0.066	0.089
$\tau_{1L}$ (s)	$\tau_{2L}$ (s)	$\tau_{3L}$ (s)	$\tau_{4L}$ (s)	$\tau_{5L}$ (s)
0.6	6	30	60	300

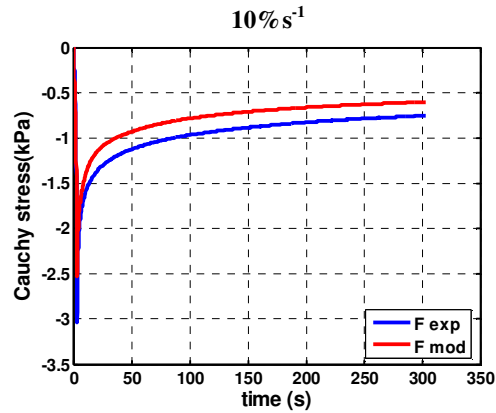
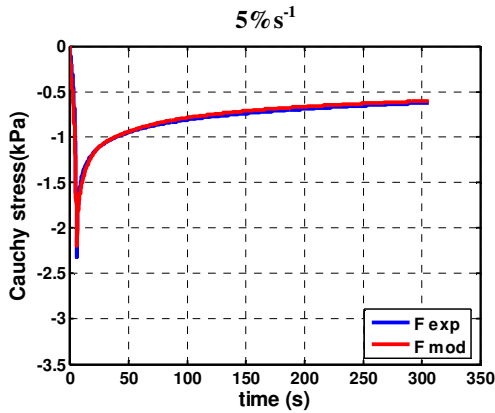
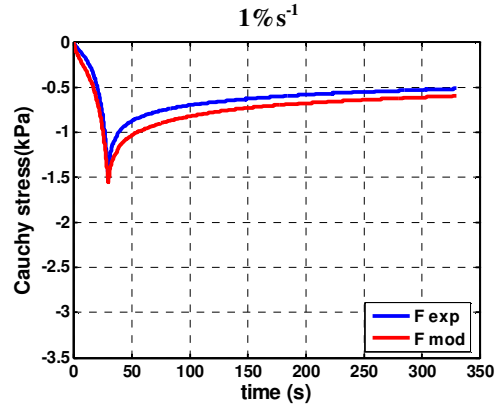
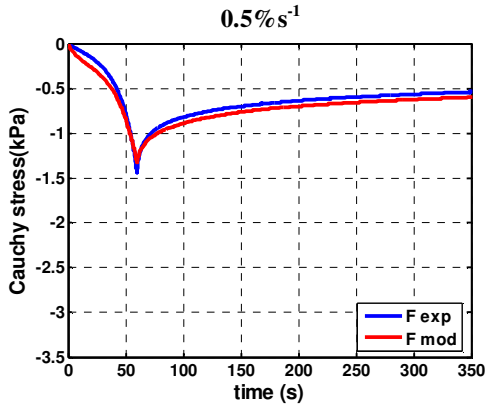
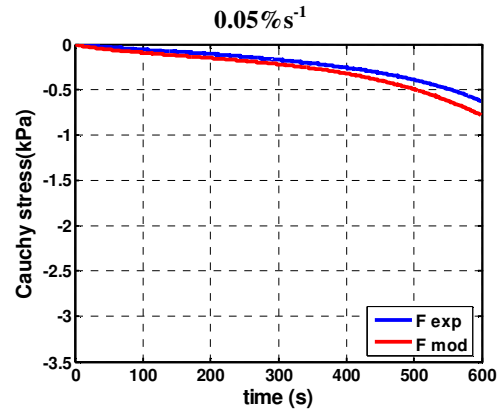


Figure 7: Comparison between experimental stress-relaxation results (—) and viscoelastic SYM model fitting (—) in fibre direction. Simultaneous fitting to data at 0.5, 1 and 10% s<sup>-1</sup>.

Cross-fibre direction

Parameters values				
-------------------	--	--	--	--

0.05% s<sup>-1</sup>

$k_{1T}$ (kPa)	$k_{2T}$ (kPa)	$k_{3T}$ (kPa)	-	-
1.293	0.911	10.869		
$p_{1T}$	$p_{2T}$	$p_{3T}$	$p_{4T}$	$p_{5T}$
0.467	0.120	0.026	0.100	0.056
$\tau_{1T}$ (s)	$\tau_{2T}$ (s)	$\tau_{3T}$ (s)	$\tau_{4T}$ (s)	$\tau_{5T}$ (s)
0.6	6	30	60	300

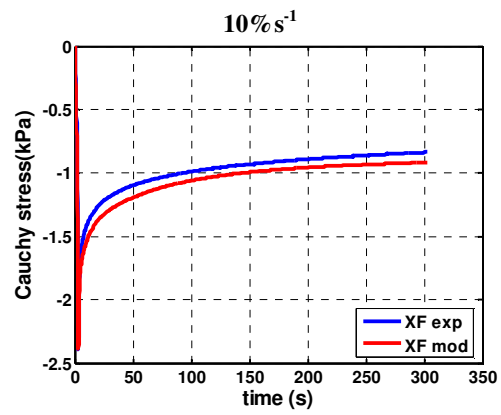
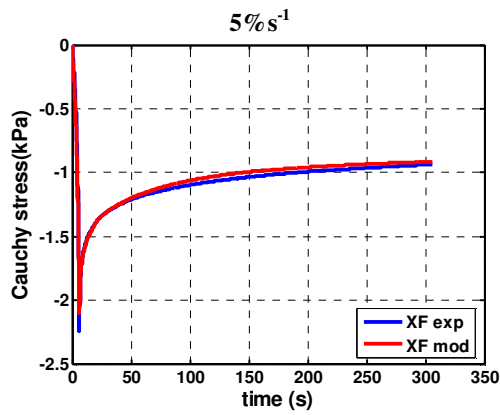
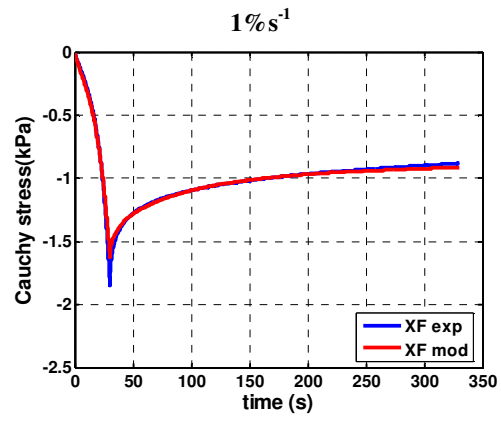
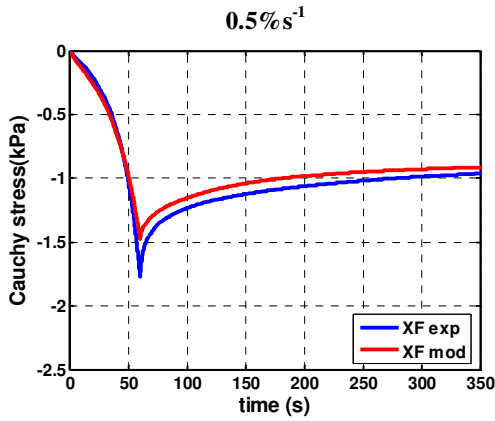
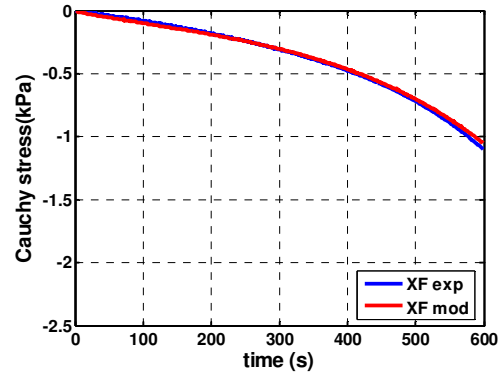


Figure 8: Comparison between experimental stress-relaxation results (—) and viscoelastic SYM model fitting (—) in cross-fibre direction. Simultaneous fitting to data at 0.5, 1 and 10%  $s^{-1}$ .

(a)

(b)

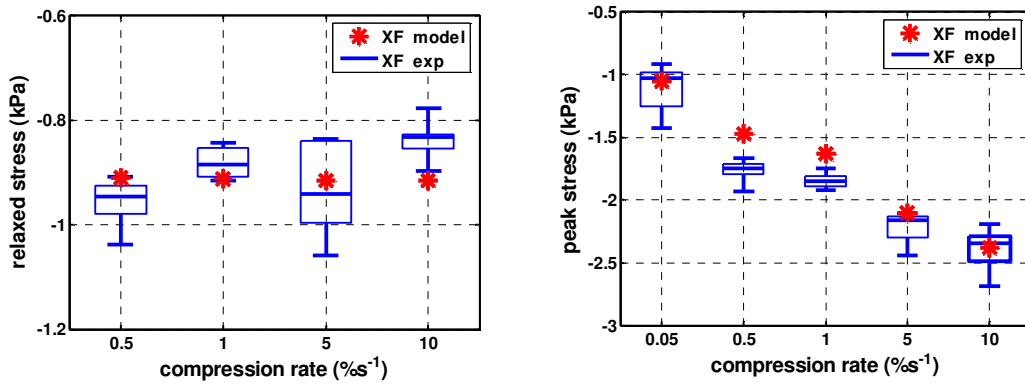


Figure 9: Comparison between experimental and theoretical relaxed stresses. Box and whiskers correspond to experimental values; Stars represent theoretical values.

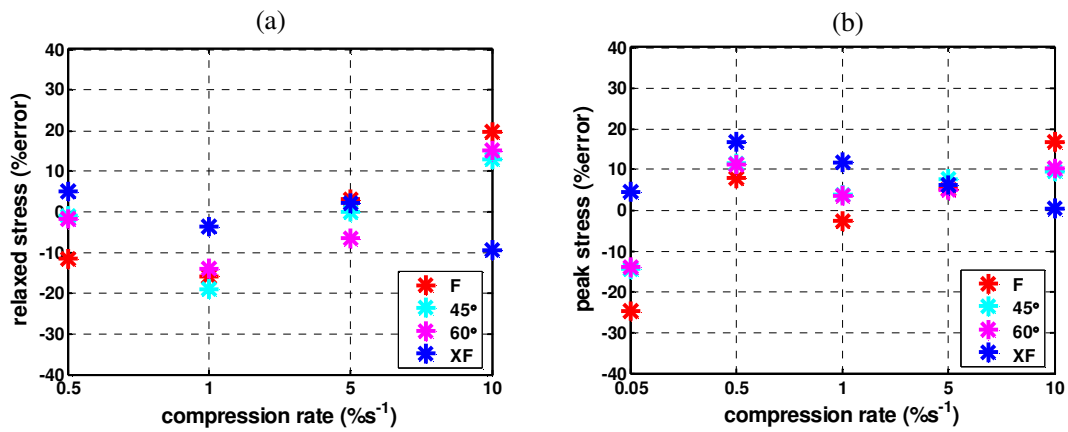


Figure 10: percentage errors between theoretical and experimental (a) relaxed stresses, (b) peak stresses at all rates and fibre orientations considered (unidirectional approach).

60° from the fibre direction – model predictions  
0.05% s<sup>-1</sup>

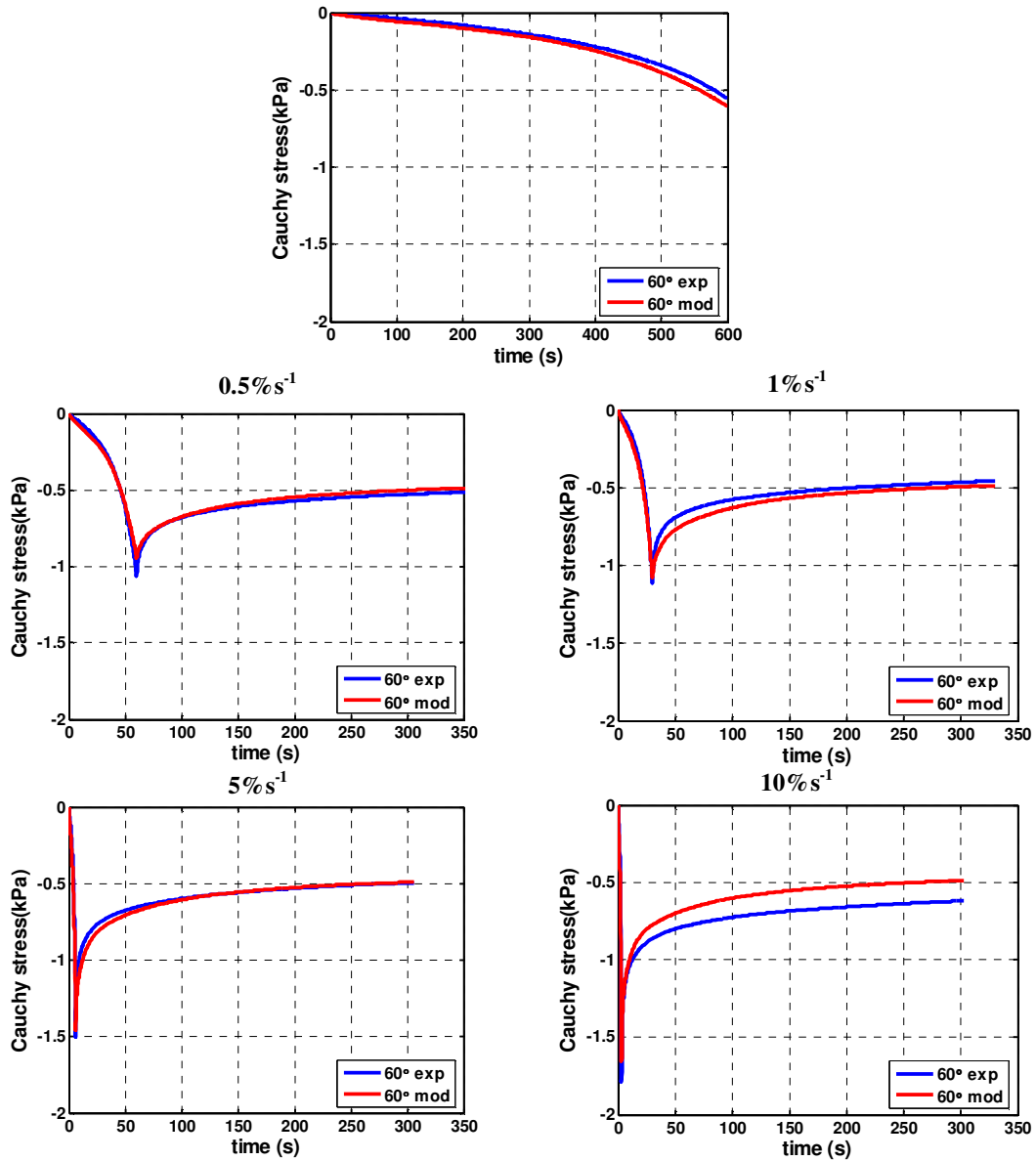
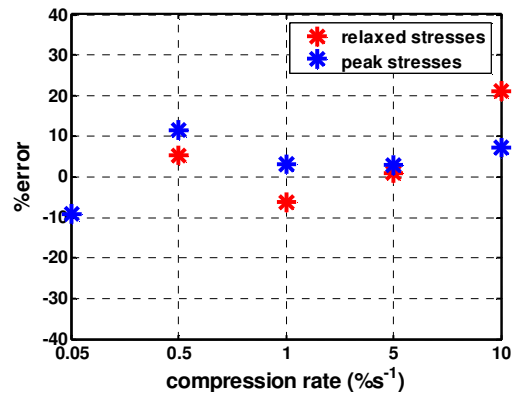
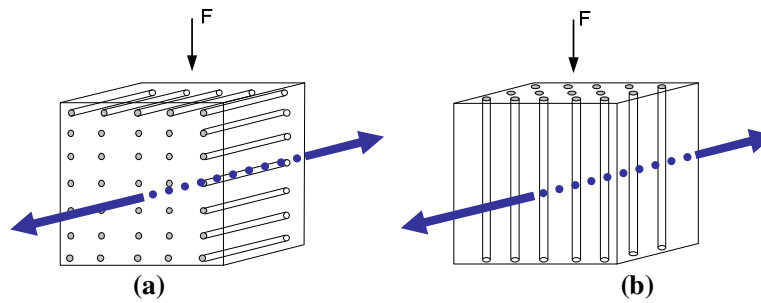


Figure 11: Comparison between experimental stress-relaxation results (—) and viscoelastic SYM model predictions (—) at 60° from the fibre direction.



**Figure 12: percentage errors between theoretical and experimental (a) relaxed stresses, (b) peak stresses at 60° from the fibre direction.**



**Figure 13: Illustration of the influence of the fluid component on muscle viscoelastic behaviour during compression in (a) cross-fibre and (b) fibre directions.**